Scientific Research Journal,
Vol 22, No 1 (2025) 19-37
https://doi.org/10.24191/srj.v22i1.17028

Performance of Spent Iron-Based Catalyst in the Photo Assisted Electrochemical System for the Removal of Methylene Blue (MB) Dye

Nurul Athikah Azizan[1], Norhaslinda Nasuha[1,*], Hawaiah Imam Maarof[1], Wan Izhan Nawawi Wan Ismail[2], Suriati Sufian[3], Nurul Izzah Ahmad Shakri[1], Nadiatul Nabilah Zahar[1]

[1]School of Chemical Engineering, College of Engineering, Universiti Teknologi MARA, 40450 Selangor, Malaysia
[2]Faculty of Applied Sciences, Universiti Teknologi MARA, 02600 Arau, Perlis, Malaysia
[3]Chemical Engineering Department, Universiti Teknologi PETRONAS, Bandar Sri Iskandar, 32610 Sri Iskandar, Perak, Malaysia

[*]Corresponding Author's E-mail: norhaslinda.nasuha@uitm.edu.my

Received: 21 November 2024
Accepted: 12 January 2025
Online First: 01 March 2025

ABSTRACT

This study explores the efficacy of a spent iron-based (Fe.S) catalyst for the photo-assisted electrochemical for removal of Methylene Blue (MB) dye. The catalyst performance was assessed under various operational parameters, including catalyst loading, initial solution pH, current density, and initial dye concentration. The commercial iron oxide (Fe_3O_4) performance was benchmarked against spent iron-based catalyst under similar operational conditions. The results revealed that the best catalyst dosage was found at 0.02 g and 0.06 g for Fe.S and Fe_3O_4, respectively. Interestingly, the Fe.S achieved complete MB decolorization, surpassing Fe_3O_4 which only reached 75% under similar conditions. To support these comparative performances, the catalysts were characterized using SEM-EDX, XRD, FTIR, and BET analyses. After five cycles of reusability, the Fe.S maintained complete removal of MB, whereas the Fe_3O_4 reusability maintained 45% after three cycles. However, Fe.S experienced leaching of metal ions concentration range 0.1 – 0.5 mgL^{-1}, which is exceed the allowable regulatory limits. Overall, the study highlights the potential of Fe.S for efficient MB dye removal. Nonetheless, the metal leaching concern must be resolved prior to practical application.

Keywords: Photo-electrochemical; Spent Iron Catalyst; Pollutant Remediation; Methylene Blue; Catalyst Stability

INTRODUCTION

Synthetic organic dyes are extensively utilized in various industries, including textile manufacture, paper production, and clothing [1]. Additionally, some dyes serve as pharmaceutical precursors and laboratory indicators. However, the extensive use of these compounds poses significant environmental and human health risks due to inherent toxicity and carcinogenicity, even at low concentrations [2]. Conventional physicochemical and biological water treatment methods have proven inadequate for the removal of these recalcitrant organic dyes [2]. Consequently, the development of effective, on-site treatment technologies is imperative for mid-sized industries [2]. The textile and pharmaceutical industries utilize materials composed of metals and synthetic organic and inorganic compounds, which pose significant environmental and health risks [3]. Methylene blue (MB), a widely used cationic dye, is of particular concern due to its toxicity, carcinogenicity, and environmental persistence [3]. The MB is resistance to degradation of light, heat, water, and oxidation hinders the effective treatment of contaminated effluents [4]. Consequently, aquatic organisms and humans may be exposed to harmful levels of this pollutant. Even at low concentrations (< 1 ppm), MB can impart a noticeable color change to water bodies [4].

Advanced oxidation processes (AOPs) are innovative methods for eliminating recalcitrant organic pollutants in water through the in-situ generation of highly reactive hydroxyl radicals (•OH) [5,6]. Technically, these AOPs method are frequently integrated with other processes such as biological oxidation to enhance contaminant removal [7]. Alternatively, AOPs can be classified into photocatalytic [8-9], electrocatalytic [10-11], and photoelectrocatalytic oxidation [12-13]. Nevertheless, AOPs which often suffer from limitations such as low efficiency, high energy consumption, and the generation of harmful by-products, photoelectrochemical advanced oxidation processes (PEOPs) are emerging as promising techniques for wastewater remediation, outperforming traditional AOPs in terms of adaptability, efficiency, and environmental compatibility. Generally, photocatalytic oxidation used light energy to generate oxidizing agents,

while electrocatalytic oxidation used electrical energy [14]. These methods leverage photocatalysts to generate charge carriers, which subsequently induce the formation of reactive oxygen species such as •OH and superoxide ions ($O_2^{\bullet-}$). These highly oxidizing intermediates facilitate the degradation of organic contaminants in wastewater as shown in Equation (1) and Equation (2) [15].

$$M + H_2O \rightarrow M(\bullet OH) + H^+ + e^- \quad (1)$$

$$M(\bullet OH) + R \rightarrow M + Intermediates \rightarrow CO_2 + H_2O + Inorganic\ ions \quad (2)$$

The PEAOPs methods are eco-friendly techniques surpass the advanced oxidation processes in several key areas. These methods exhibit exceptional adaptability, efficiency, and compatibility with the environment. The anodic materials categorized as either active, with low O_2 overpotential, or non-active, with high O_2 overpotential, have demonstrated efficacy in catalyzing H_2O oxidation to generate •OH radicals, which subsequently oxidize organic compounds [15]. Their broad applicability and effectiveness in pollutant removal make them promising solutions for environmental remediation [12]. Titanium dioxide (TiO_2) is a prominent photocatalyst for pollutant degradation and photoelectrochemical processes under solar illumination due to its robust redox properties, exceptional photochemical stability, and non-toxicity [16]. Nevertheless, its wide bandgap and rapid charge carrier recombination hinder light adsorption and overall efficiency [17].

Mixed-metal oxides (MMOs) exhibit promising potential for the degradation of environmental pollutants in air and water streams [18]. The MMOs catalytic activities can facilitate the conversion of harmful contaminants into less harmful or non-toxic products [19]. Additionally, MMOs play a crucial role in various synthetic processes, including the selective production of fuels, polymers, and high-value chemicals [20]. Their ability to promote specific reaction pathways while minimizing by-products makes them ideal for efficient chemical manufacturing [20]. Albeit the MMOs containing valuable or rare earth metals, improper disposal of MMOs can lead to environmental pollution such as soil and groundwater pollutions due to the metals leaching out over time, posing a threat to human health and ecological systems. Therefore, the MMOs waste could

potentially be recycled and used in new applications, for instance, as a catalyst, electrochemical materials, sensors, and others [19]. However, the MMOs shows great promise as a catalyst for organic pollutant degradation, hence continued research efforts to address current benefits and limitations will pave the way for its adoption in wastewater treatment and environmental clean-up technologies. Recent developments established the utilization of metal-waste as catalysts for degradation of organic pollutants such as magnetic waste iron slag composite (MIS) [21], iron rich waste in fly ash (FA), foundry sand (FS), red mud (RM), and blast sand (BS) [22], FeO-constituted iron slag (IS) [23], Fe_3O_4-carbon nanocomposite [24], Fe_3O_4@C incorporated MIL-53(Fe) [10], and $Fe_3O_4/NiFe_2O_4$ nanocomposite derived from iron rust waste [25].

This study investigates the catalytic activity of iron sludge in the photoelectrochemical (PEC) degradation of methylene blue. The photoelectrocatalysis is an advanced oxidation process that surpasses conventional electrochemical degradation by mitigating flocculation and harmful by-products formation. This enhancement is attributed to the synergistic effect of photogenerated holes (h^+), ($O_2^{\bullet-}$), and ($^{\bullet}OH$) on the photocatalyst surface. Thus, the PEC technology harnesses light energy to induce redox reactions via electron-hole pair generation within a semiconductor material, such as iron sludge. Based on the reusability tests, the Fe.S catalyst is unstable due to metal leaching for prolonged use in photoelectrochemical advanced oxidation processes.

EXPERIMENTAL METHODOLOGY

Chemicals

In this investigation, methylene blue (MB, RMStain, R&M) was employed as a model pollutant. Its physicochemical properties are tabulated in Table 1. A stock solution of MB, with a concentration of 200 ppm was prepared. Sodium chloride (NaCl, Fisher Chemical) solution was used as a supporting electrolyte. The pH of the solution was adjusted to the desired level using 0.1 M of sodium hydroxide (NaOH, Pellet, R&M Chemicals) and hydrochloric acid (HCl, 37%, Fisher Scientific).

Table 1: Specification of MB dye.

Properties	
Chemical name	3,7-Bis(dimethylamino)phenothiazin-5-ium chloride trihydrate
Common name	Methylene Blue
Generic name	Basic Blue 9
CAS number	7220-79-3
Color index number	52015
Ionisation	Basic
Solubility	Soluble in water: 50 g L^{-1} at 25 °C
λ_{max}	668 nm
Empirical formula	$C_{16}H_{18}ClN_3S_3H_2O$
Molecular weight	373.9 g mol^{-1}

Preparation of spent iron-based catalyst (Fe.S)

Iron sludge was transformed into a catalyst through a multi-step process as shown in Figure 1. Initially, the raw iron sludge was sieved to a particle size of 40-50 µm to eliminate debris and rocks. The sieved material was then subjected to repeated steps of washing and filtration to eliminate impurities and fine particles. The washed sludge was then dried overnight in an oven at 80 °C before undergoing calcination at 450 °C in a furnace to form iron oxide.

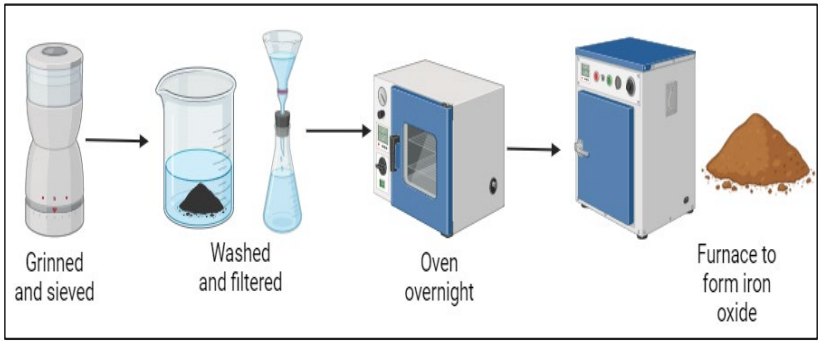

Figure 1: Preparation of Fe.S catalyst.

Catalytic performance for removal of methylene blue via photoelectrochemical method

The procedure was adapted from Muin *et al.* [26] studies. A 100 mL of aqueous solution containing 50 ppm of MB dye was prepared and mixed with the catalyst. The solution was maintained in darkness for 20 minutes to establish an adsorption/desorption equilibrium prior to ultraviolet lamp exposure. To enhance current density, a few drops of 1 M NaCl were added. A platinized titanium anode and a carbon cathode was immersed in the solution. The dye solution was stirred at 160 rpm for 3 hours. Timekeeping commenced immediately upon NaCl addition. A direct current (DC) power supply was connected to provide a constant current of 4 mA/cm2. The experiment was conducted at the initial pH of the MB solution. Each experimental condition was replicated thrice. A schematic representation of the experimental setup is presented in Figure 2.

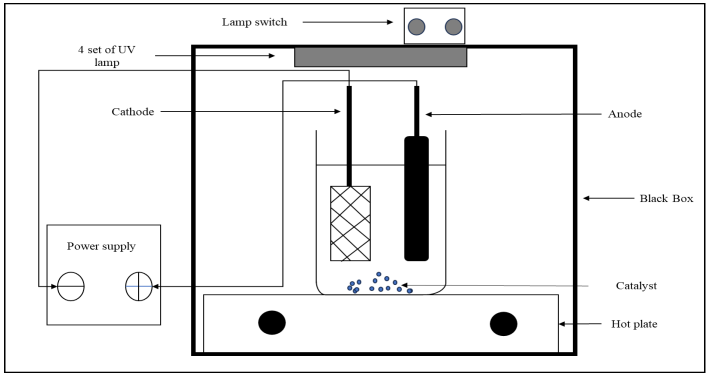

Figure 2: Schematic diagram of experimental setup.

To elucidate optimal experimental conditions, several parameters were investigated: i) Fe.S loading (0.01 to 0.06 g), ii) initial pH of MB (pH 2 to 7), iii) initial MB concentration (25 to 150 ppm), iv) catalyst reusability, and v) metal leaching. The percentage of MB removal was determined using Equation (3).

$$\% \text{ Removal} = \frac{[C]_i - [C]_f}{[C]_i} \times 100\% \quad (3)$$

where C_i and C_f(mg L^{-1}) are the liquid phase concentration of dyes at initial and final stage, respectively.

Analytical method

Reusability

The stability and reusability of Fe.S catalyst were evaluated through several consecutive removal cycles of MB under optimal reaction condition. Experimental parameters, including initial dye concentration (50 ppm), pH 6, and treatment time (120 minutes), were maintained constant throughout the study. After each photoelectrochemical cycle, the catalyst was washed and dried in the oven for 1 hour at 60 °C to remove dye residue.

Metal leaching

The concentration of leached metal ion in the reaction supernatant were determined using Inductively Coupled Plasma Optical Emission Spectroscopy (ICP-OES, Optima 7000DV, PerkinElmer), employing a quality control standard with 21 elements in a 5% HNO_3 matrix. The Fe.S catalyst's stability was correlated to the extent of metal ion leaching into the bulk solution during the reaction.

RESULTS AND DISCUSSION

Figure 3(a) reveals the rough, uneven surface and porous structure characteristic of Fe.S catalysts produced via thermal decomposition. The catalyst exhibits a broad size distribution and hierarchical clustering of primary nanoparticles into larger agglomerates. In contrast, Figure 3(b) shows commercial Fe_3O_4 possess a cubic inverse spinel crystal structure, incorporating both Fe^{2+} and Fe^{3+} ions [27]. However, the Fe_3O_4 can be synthesized into nanoparticles, resulting in a uniform size distribution and enhanced surface-to-volume ratio [28]. A study demonstrates the potential of thermally treated iron-containing sludge to serve as a heterogeneous catalyst for the efficient degradation of dye pollutants. This catalyst exhibits notable catalytic activity in both homogeneous and heterogeneous reactions, particularly for the removal of 4-chlorophenol [29-30].

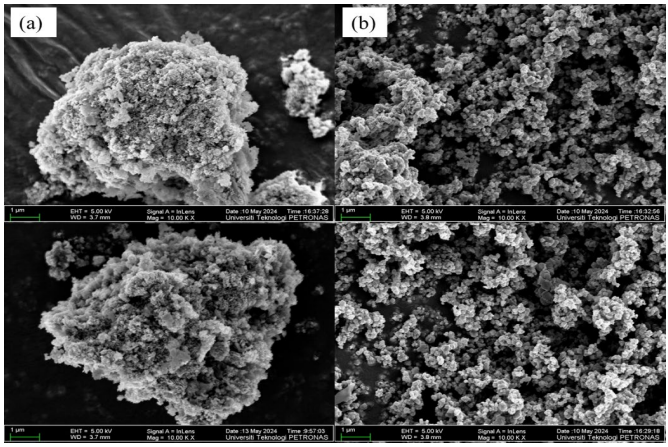

Figure 3: SEM of (a) Fe.S and (b) Fe_3O_4.

Effect of catalyst dosage

Figure 4 illustrates a distinct relationship between catalyst loading and MB removal efficiency over time. At lower or higher catalyst loading from 0.01 to 0.06 g, the removal efficiencies exhibit a complete decolorization within 30 minutes. Furthermore, the implementation of photoelectrochemical process in this study demonstrated that while increasing the catalyst loading initially enhanced MB removal, there was a threshold beyond which further increases did not significantly improve removal efficiency. However, higher catalyst loadings resulted in diminishing returns, suggesting that excessive catalyst can lead to aggregation, thereby reducing the effective surface area available for redox reactions [31]. According to Ikhlaq *et al.* [31], experiments employing alum as a catalyst in ozonation process revealed that increasing the alum loading, MB decolorization improved to almost complete color removal. Accordingly, increasing catalyst loading generally results in improved removal efficiencies up to a particular limit. Beyond this limit, removal efficiency may plateau or even decrease due to factors for instance, reduced active surface area and increased competition among dye molecules for reactive sites [32].

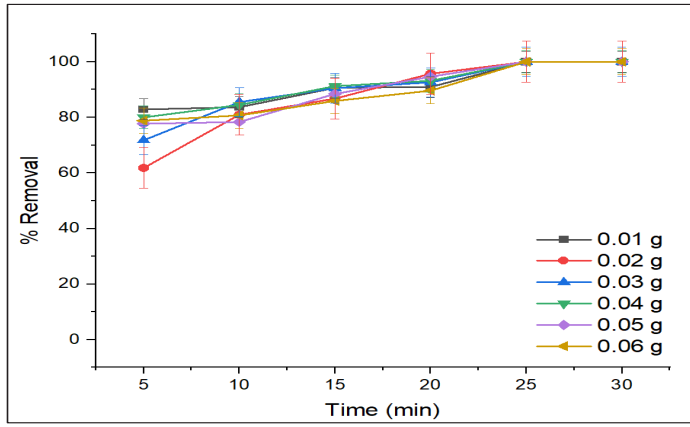

Figure 4: Effect of catalyst dosage at [MB]: 50 mg/L, pH 5, current density 0.4 A/m², 30 min treatment time.

Effect of methylene blue initial concentration

The influence of initial concentration on the decolorization of MB was investigated by varying the MB concentrations to 25, 50, 75, 100, 125, and 150 ppm. The decolorization of MB was investigated under fixed experimental conditions: catalyst dosage of 0.01 g and pH of 5. The correlation between MB initial concentration and decolorization efficiency is illustrated in Figure 5. A significant observation was that increasing the initial concentration of dyes had a negligible influence on the decolorization efficiency of the dyes. The methylene blue dye exhibited complete color removal at both low and high initial concentrations. After 30 minutes of treatment time, the rate of color removal began to plateau, resulting in marginal improvement. This is due to the loss of active species from the iron-sludge catalyst surface during electrochemical process. The oxidation of an active species via an electrochemical reaction with water and its components, which are transferred into the treated medium, ultimately resulting in catalyst deactivation [33].

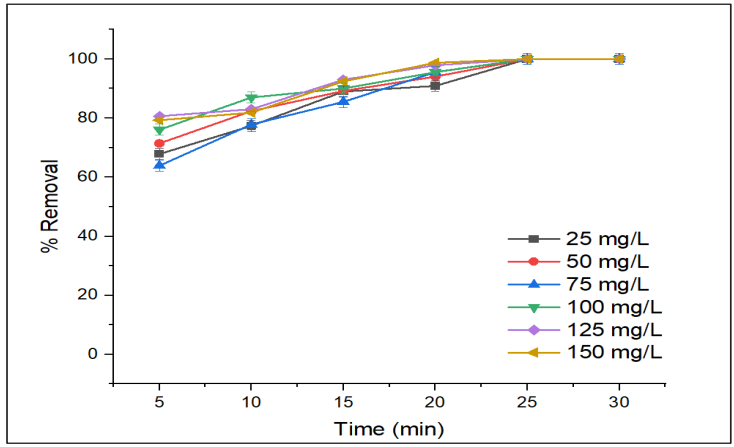

Figure 5: Effect of MB initial concentration at pH 5, current density 0.4 A/m², 30 min treatment time.

Effect of initial pH

The effect of pH is a vital parameter in photoelectrochemical process. To evaluate the impact of pH on MB dye degradation efficiency, the MB concentration was kept constant throughout the experiment at 50 ppm and catalyst dosage at 0.01 g while manipulated the pH (2, 3, 4, 5, 6, and 7). The pH not only influences adsorption capacity but also affects the degradation mechanisms. For instance, at different pH levels, the relative contributions of photolysis and oxidation to MB degradation can vary, impacting the overall removal efficiency. Figure 6 demonstrates that at pH 5 and 6, which initial pH of MB, the removal efficiency rapidly increases, reaching nearly complete decolorization within 30 minutes. This superior performance can be attributed to favorable surface charge interactions between the iron-sludge catalyst and MB molecules at this pH level. However, at pH values ranging 2 to 7, complete substrate removal of MB was observed, and the removal efficiency remains constant after 30 minutes. Moreover, different studies have shown that an optimal pH ranges for utmost MB removal efficiency. According to Alkayal *et al.* [34], the experiment employing palladium nanoparticles exhibit the degradation efficiency of MB was observed to be the highest at slightly acidic to neutral pH levels, specifically at pH 5 and 6.6, reaching degradation efficiencies of 98.1% and 99.6%, respectively.

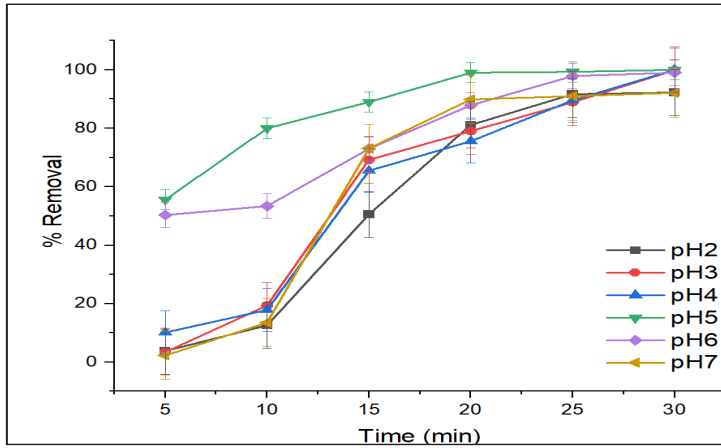

Figure 6: Effect of initial pH at [MB]: 50 mg/L, current density 0.4 A/m², 30 min treatment time.

Comparison of iron-sludge (Fe.S) catalyst and commercialized iron (III) oxide (Fe_3O_4)

Based on Figure 7, iron sludge exhibits better performance with utmost MB degradation compared to commercialised iron oxide. This is due to the iron sludge has been shown to be an effective heterogeneous catalyst for the degradation of organic dyes, often requiring a lower dosage compared to commercial iron (III) oxide. According to Adachi *et al*. [35], has found that the superior catalytic performance of iron-doped hydrochar (5% Fe@ BC) for the removal of methyl orange dye in a heterogeneous Fenton-like process. Notably, this catalyst requiring a lower catalyst dosage and hydrogen peroxide compared to alternative materials such as cobalt ferrite and copper ferrite. The removal of methylene blue using Fe.S catalyst and Fe3O4 under different pH conditions has been explored in various studies. Based on Figure 7, iron sludge catalyst worked better, especially at a pH of 5, which removed up to 98% of MB, while Fe_3O_4 only removed 47% at a pH of 2. Furthermore, iron sludge catalyst exhibits higher MB removal efficiency from lower to higher concentrations with 0.01 g of catalyst dosage. However, Fe_3O_4 used 0.06 g of catalyst dosage to efficiently removal MB for both lower and higher concentrations. A study investigates the influence of catalyst dosage on the dye removal. While increasing the catalyst dosage generally enhances adsorption and removal efficiency, there exists an

optimal loading beyond which further increases, resulting in decreased performance due to nanoparticles aggregation, leading to a reduction in the number of available active sites [36]. These findings suggest the importance of optimizing catalyst dosage for effective dye removal.

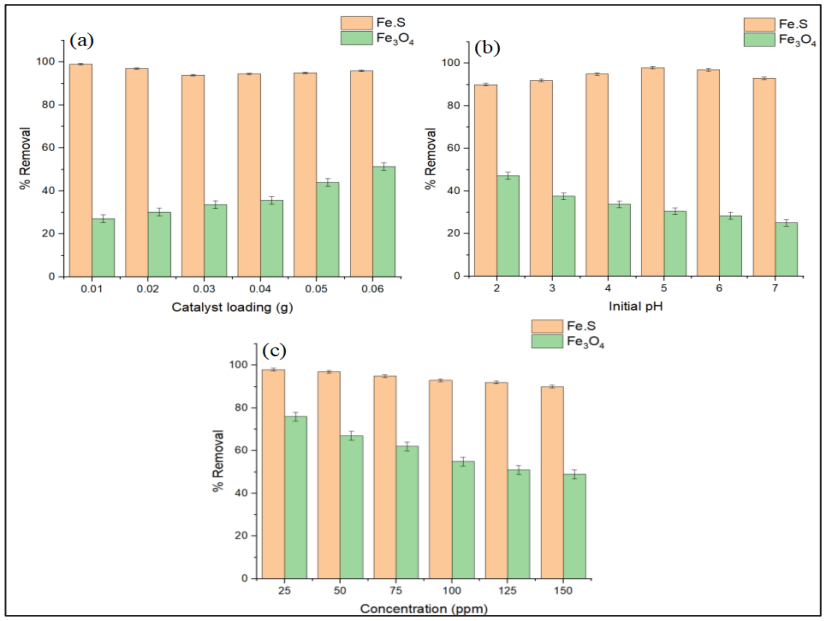

Figure 7: Comparison of Fe.S and Fe_3O_4 catalyst, (a) Effect of catalyst loading, (b) Effect of initial pH, and (c) Effect of initial concentration at current density 0.4 A/m^2, 30 min treatment time.

Reusability

The reusability of Fe.S and Fe_3O_4 catalysts were investigated for decolorization of methylene blue at a concentration of 50 ppm and at a pH of 6 and 2 for Fe.S and Fe_3O_4, respectively. The catalytic performance was evaluated over five consecutive cycles to assess its durability and potential for long-term applications in wastewater treatment. Additionally, Fe.S catalysts demonstrated higher reusability compared to Fe_3O_4, maintaining nearly complete decolorization of MB for five consecutive runs. The catalytic activity of Fe_3O_4 significantly decreased after repeated used, resulting in drastically dropped to 48% of MB decolorization efficiency. Unfortunately, Fe.S catalyst exhibited metal leaching into dye solution during consecutive

reuse cycles. The leaching level ranged from 0.1 to 0.5 mg/L, exceeding allowable regulatory limits. The leaching of metal ions from catalyst can alter the catalyst surface properties, affecting the dye removal capacity. For instance, iron-based catalyst exhibit varying performance depending on the metal content and the presence of competing ions. When metal ions leached into the solution, they can interact with dye molecules, potentially forming complexes that hinder effective dye removal [37]. These findings indicate that iron sludge catalyst requires modification to mitigate metal leaching. Additionally, a comparative study reveals the superior catalytic performance of Fe.S catalysts relative to conventional Fe_3O_4. These sludge-based catalysts show remarkable durability, maintaining approximately 90% pollutant removal efficiency even after multiple catalytic cycles [29]. These findings suggest promising implications for the development of sustainable and effective wastewater treatment processes utilizing iron sludge-derived catalysts.

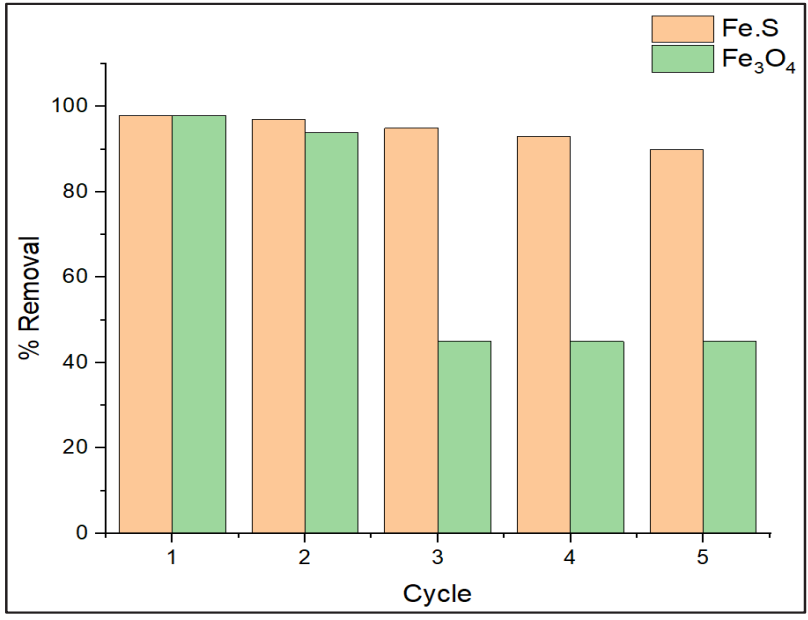

Figure 8: Reusability of catalyst Fe.S and Fe_3O_4 at [MB]: 50 mg/L, pH 5, current density 0.4 A/m², 30 min treatment time.

CONCLUSION

Synthesized Fe.S exhibits significantly enhanced catalytic properties compared to commercial Fe_3O_4. This superior catalytic performance is primarily attributed to its heterogeneous composition containing a variety of active metal oxides and a porous structure. The latter provides a larger surface area, facilitating enhanced reactant adsorption and product desorption, thereby accelerating catalytic reaction. In conclusion, the Fe.S catalyst exhibited exceptional catalytic activity for the photoelectrochemical degradation of MB compared to commercial Fe_3O_4. Optimal operational conditions were determined, including a catalyst dosage of 0.01 g and a pH of 5, resulting in near-complete degradation within 30 minutes. These findings highlight the critical role of fine-tuning operational parameters in maximizing catalytic efficiency and promoting the application of iron sludge-based catalysts in sustainable wastewater treatment. Nevertheless, the phenomenon of metal leaching must be mitigated to ensure its viability before practical applications. One potential strategy involves the synthesis of metal-organic frameworks (MOFs) incorporating Fe.S. By encapsulating Fe.S within the MOFs matrix, the leaching of metal ions can be significantly suppressed, thereby enhancing the structure and stability of the catalyst.

ACKNOWLEDGEMENTS

We would like to thank Assoc. Prof. Dr. Suriati Sufian from Universiti Teknologi PETRONAS for conducting the SEM measurements and Assoc. Prof. Dr. Wan Izhan Nawawi Wan Ismail from Universiti Teknologi MARA, Perlis, for performing the ICP-OES measurements. This research was conducted independently without any external financial support. We would like to express our sincere gratitude to all those who contributed to this research. Their support and encouragement were instrumental in the successful completion of this study.

REFERENCES

[1] V. Hegde, U.T. Uthappa, O.R. Arvind Swami, S.S. Han, and H.Y. Jung, 2022. Sustainable green functional nano aluminium fumarate-MOF decorated on 3D low-cost natural diatoms for the removal of Congo red dye and fabric whitening agent from wastewater: Batch & continuous adsorption process, *Material Today Communications*, 32(6), 103887.

[2] A.L. Magdaleno, E. Brillas, S. Garcia-Segura, and A.J. dos Santos, 2024. Comparison of electrochemical advanced oxidation processes for the treatment of complex synthetic dye mixtures, *Separation and Purification Technology*, 345, 124758.

[3] G.Z. Girotto, A.S. Thill, L.P. Matte, M.A.H. Vogt, and T.V. Machado, 2022. Ni/$SrTiO_3$ nanoparticles for photodegradation of methylene blue, *ACS Applied Nano Materials*, 5(2), 1825 – 1832.

[4] Z. McCaffrey, L.F. Torres, B.-S. Chiou, W. Hart-Cooper, and C. McMahan, 2024. Almond and walnut shell activated carbon for methylene blue adsorption, *ACS Sustainable Resources Management,* 1(4), 1421 – 1431.

[5] A. Magomedova, A. Isaev, and F. Orudzhev, 2024. Oxygen vacancies enhanced photo-Fenton-like catalytic degradation of Rhodamine B by electrochemical synthesized α-Fe_2O_3 nanoparticles, *Inorganic Chemistry Communications*, 165, 108229.

[6] H. Luo, Y. Zeng, D. He, and X. Pan, 2021. Application of iron-based materials in heterogeneous advanced oxidation processes for wastewater treatment: A review, *Chemical Engineering Journal*, 407, 127191.

[7] H.R. Dihom, M.M. Al-Shaibani, R.M.S. Radin Mohamed, and A.A. Al-Gheethi, 2022. Photocatalytic degradation of disperse azo dyes in textile wastewater using green zinc oxide nanoparticles synthesized in plant extract: A critical review, *Journal of Water Process Engineering,*

47, 102705.

[8] A. Zarandona, H. Salazar, M. Insausti, S. Lanceros-Méndez, and Q. Zhang, 2024. Synergistic green degradation of organic dyes using a BiSI catalyst: Adsorption, sonocatalysis, and photocatalysis, *Journal of Water Process Engineering*, 58, 104893.

[9] R. Behura, R. Sakthivel, and N. Das, 2021. Synthesis of cobalt ferrite nanoparticles from waste iron ore tailings and spent lithium-ion batteries for photo/sono-catalytic degradation of Congo red, *Powder Technology,* 386, 519 – 527.

[10] M. Priyadarshini, A. Ahmad, and M.M. Ghangrekar, 2023. Efficient upcycling of iron scrap and waste polyethylene terephthalate plastic into Fe_3O_4@C incorporated MIL-53(Fe) as a novel electro-Fenton catalyst for the degradation of salicylic acid, *Environmental Pollution,* 322, 121349.

[11] G. Huang, L. Zhao, S. Yuan, N. Li, and S. Jing, 2022. Iron doped mesoporous cobalt phosphide with optimized electronic structure for enhanced hydrogen evolution, *International Journal of Hydrogen Energy,* 47(31), 14767 – 14776.

[12] M.G. Kim, J.E. Lee, K.S. Kim, J.M. Kang, and J.H. Lee, 2021. Photocatalytic degradation of methylene blue under UV and visible light by brookite-rutile bi-crystalline phase of TiO_2, *New Journal of Chemistry*, 45(7), 3485 – 3497.

[13] G. Yanagi, M. Furukawa, I. Tateishi, H. Katsumata, and S. Kaneco, 2022. Electrochemical decolorization of methylene blue in solution with metal-doped Ti/α,β-PbO_2 mesh electrode, *Separation Science and Technology,* 57(2), 325 – 337.

[14] J.A. Khan, M. Sayed, N.S. Shah, S. Khan, and Y. Zhang, 2020. Synthesis of eosin-modified TiO_2 film with co-exposed {001} and {101} facets for photocatalytic degradation of para-aminobenzoic acid and solar H2 production, *Applied Catalysis B: Environmental,*

265, 118581.

[15] B. G, F. Banat, and M. Abu Haija, 2023. Photoelectrochemical advanced oxidation processes for simultaneous removal of antibiotics and heavy metal ions in wastewater using 2D-on-2D WS2@$CoFe_2O_4$ heteronanostructures, *Environmental Pollution*, 339, 122753.

[16] M.A. Acosta-Esparza, L.P. Rivera, A. Pérez-Centeno, A. Zamudio-Ojeda, and D.R. González, 2020. UV and visible light photodegradation of methylene blue with graphene-decorated titanium dioxide, *Materials Research Express*, 7(1), 015504.

[17] A. Zulkiflee, M. Mansoob Khan, M. Yusuf Khan, A. Khan, and M. Hilni Harunsani, 2024. Nb_2O_5/BiOCl composite as a visible-light-active photocatalyst for the removal of RhB dye and photoelectrochemical studies, *Journal of Photochemistry and Photobiology A: Chemistry,* 446, 115177.

[18] P. Kaur, M.A. Khan, Y. Li, A.A.S. Al-Othman, and Z.A. Alothman, 2023. Investigating the effectiveness of bifacial mixed metal MOF electrodes for the photoelectro-catalytic treatment of municipal wastewater, *Journal of Cleaner Production,* 392, 136273.

[19] N.A. Johari, N. Yusof, and A.F. Ismail, 2022. Performance of mixed matrix ultrafiltration membrane for textile wastewater treatment, *Materials Today: Proceedings*, 65, 3015 – 3019.

[20] N.T. Nhan, and T. Le Luu, 2023. Fabrication of novel Ti/SnO_2-Nb_2O_5 electrode in comparison with traditional doping metal oxides for electrochemical textile wastewater treatment, *Environmental Technology & Innovation,* 32, 102194.

[21] L.H. Nguyen, H.T. Van, Q.N. Ngo, V.N. Thai, and V.H. Hoang, 2021. Improving Fenton-like oxidation of Rhodamine B using a new catalyst based on magnetic/iron-containing waste slag composite, *Environmental Technology & Innovation*, 23, 101582.

[22] Y. Pandey, A. Verma, and A.P. Toor, 2023. Abatement of paraquat-contaminated water using solar-assisted heterogeneous photo-Fenton-like treatment with iron-containing industrial wastes as catalysts, *Journal of Environmental Management*, 325, 116550.

[23] H.T. Van, L.H. Nguyen, T.K. Hoang, T.P. Tran, and A.T. Vo, 2019. Using FeO-constituted iron slag wastes as a heterogeneous catalyst for Fenton and ozonation processes to degrade Reactive Red 24 from aqueous solution, *Separation and Purification Technology,* 224, 431– 442.

[24] J. Samuel, A. Shah, D. Kumar, L. Robindro Singh, and M. Mahato, 2021. Preparation, characterization, and some electrochemical study of waste-derived iron oxide-carbon nanocomposite, *Materials Today: Proceedings*, 47, 1048 –1053.

[25] I. Fatimah, I. Yanti, H.K. Wijayanti, G.D. Ramanda, and S. Sagadevan, 2023. One-pot synthesis of Fe_3O_4/$NiFe_2O_4$ nanocomposite from iron rust waste as reusable catalyst for methyl violet oxidation, *Case Studies in Chemical and Environmental Engineering*, 8, 100369.

[26] N.A.A. Muin, H.I. Maarof, N.A.A. Bashah, N.A. Zubir, and R. Alrozi, 2020. Electrochemical removal of copper ions using coconut shell activated carbon, *Indonesian Journal of Chemistry,* 20(3), 530–535.

[27] S. Xu, and T.R. Lee, 2021. Fe_3O_4 nanoparticles: Structures, synthesis, magnetic properties, and surface functionalization, *Applied Sciences,* 11(23), 11301.

[28] J. Li, C. Si, H. Zhao, Q. Meng, and B. Chang, 2019. Dyes adsorption behavior of Fe_3O_4 nanoparticles functionalized polyoxometalate hybrid, *Molecules,* 24(10), 1924.

[29] X. Liu, H.L. Liu, K.P. Cui, Z.L. Dai, and B. Wang, 2022. Heterogeneous photo-Fenton removal of methyl orange using the sludge generated in dyeing wastewater as catalysts, *Water (Switzerland)*, 14(4), 1293.

[30] N. A. Azizan, N. Nasuha, and H. I. Maarof, 2023. Degradation of reactive black 5 dye (RB5) using iron electrode (Fe.S) derived from iron sludge steel waste via electrochemical method, *IOP Conference Series: Earth and Environmental Science,* 1216(1), 012037.

[31] A. Ikhlaq, S. Parveen, M. Raashid, Z. Masood, and O.S. Rizvi, 2024. Methylene blue removal from aqueous solution by alum: Catalytic ozonation process, *Discover Chemistry Engineering*, 4, 104112.

[32] T.H.V. Luong, T.H.T. Nguyen, B.V. Nguyen, N.K. Nguyen, and T.Q.C. Nguyen, 2022. Efficient degradation of methyl orange and methylene blue in aqueous solution using a novel Fenton-like catalyst of CuCo-ZIFs, *Green Processing and Synthesis*, 11(1), 71– 83.

[33] G. Chen, Y. Zhu, S. She, Z. Lin, and H. Sun, 2024. Component leaching of water oxidation electrocatalysts, *Information Technology Materials ,* 6(11), e12609.

[34] N.S. Alkayal, M. Ibrahim, N. Tashkandi, and M.M. Alotaibi, 2023. Efficient reduction in methylene blue using palladium nanoparticles supported by melamine-based polymer, *Materials (Basel),* 16(7), 1234.

[35] A. Adachi, F. El Ouadrhiri, E.A.M. Saleh, R.H. Althomali, and A.F. Kassem, 2023. Iron-doped catalyst synthesis in heterogeneous Fenton-like process for dye degradation and removal: Optimization using response surface methodology, *Springer Nature Applied Sciences*, 5, 104456.

[36] Y.S. Jara, T.T. Mekiso, and A.P. Washe, 2024. Highly efficient catalytic degradation of organic dyes using iron nanoparticles synthesized with Vernonia amygdalina leaf extract, *Scientific Reports*, 14(4), 2890.

[37] D. Ścieżyńska, D. Bury, M. Jakubczak, J. Bogacki, and A. Jastrzębska, 2023. Waste iron as a robust and ecological catalyst for decomposition of industrial dyes under UV irradiation, *Environmental Science and Pollution Research*, 30(45), 69024 – 69041.